(Received 13 December 2023, Accepted 26 January 2024, Scheduled 9 February 2024)

A Flexible Foldable Broadband Metamaterial Absorber Fabricated by Intaglio Printing Technology

Ye Dong[1], Zhangyou Yang[2], Siqi Zhang[1,3], Rongrong Zhu[1,4], Bin Zheng[1,3], and Huan Lu[1,3,*]

[1]*International Joint Innovation Center*
Key Laboratory of Advanced Micro/Nano Electronic Devices & Smart Systems of Zhejiang
The Electromagnetics Academy at Zhejiang University, Zhejiang University, Haining 314400, China
[2]*Jiangnan Institute of Mechanical and Electrical Design Research, Guiyang 550000, China*
[3]*Jinhua Institute of Zhejiang University, Zhejiang University, Jinhua 321099, China*
[4]*School of Information and Electrical Engineering, Zhejiang University City College, Zhejiang 310015, China*

ABSTRACT: Absorbing materials can absorb incident electromagnetic waves effectively and have important research value in radar fields. However, the current absorbing materials are mostly affected by the thickness and flexibility of the dielectric substrate, and they have shortcomings such as being not thin, not flexible, not folding, and not conformal with the protection target, which is not conducive to practical application. In this paper, we propose a flexible absorbing material that can be folded freely for wearable and practical engineering applications, which is composed of a conductive carbon paste ink resistance film layer, a flexible fabric dielectric substrate, and a metal backplane. When the incidence angle is less than 30°, more than 90% absorption performance can be achieved at the operating frequency of 9.5–11.5 GHz with polarization insensitive characteristics. Simulated and experimental results prove the effectiveness of the structure. Our work provides the groundwork for the commercialization of future meta-devices such as wearable invisibility cloaks, sensors, optical filters/switchers, photodetectors, and energy converters.

1. INTRODUCTION

Electromagnetic (EM) metamaterial is an artificial composite composed of ordered or disordered subwavelength unit structures, with unique EM properties that natural materials do not have [1–8]. By varying the geometry of the artificial resonator, the metamaterial can exhibit characteristics such as the negative refractive index [9, 10], backward Cherenkov radiation [11, 12], inverse Doppler effect [13–15], and plate focusing [16–19]. In 2008, Landy et al. first proposed the concept of metamaterial perfect absorber (MPA) [20], which showed a very high absorption rate but was very thin, and can achieve impedance matching through flexible structural design and structural parameters adjustment. Compared with traditional absorbing materials, MPA has a broader development potential, so it has attracted wide attention from researchers. Thus, the research of EM metamaterials has been pushed to a new climax, and various EM metamaterials have been proposed [21–35], which play an important role in multiple fields such as photodetectors, sensors, energy harvesters, and invisible cloak [36–38] technology.

Metamaterial absorber (MA) consists of a periodically arranged metal pattern resonance layer, an intermediate dielectric layer, and a continuous metal backplane. Because most of the MAs at this stage usually choose FR4 or Rogers series plate and other hard substrates [39–41], there are shortcomings such as not being thin, not flexible, not folding, and not conformal with the protection target, which limit the practical application scenarios of MA. Although there are metamaterial absorbers made of special material resistance films such as ITO (indium tin oxide) combined with flexible dielectric substrates [42–45], it is still challenging to achieve conformal covering of complex irregular objects. Therefore, new flexible MAs need to be researched and developed urgently.

In this work, we propose a flexible MA based on intaglio printing technology. Conductive carbon paste ink and diluent are adjusted according to a specific concentration ratio to make a resistance film, and then the conductive carbon paste ink is directly printed on the flexible fabric dielectric substrate through intaglio printing technology. Compared with traditional resistance films that need to print a special material pattern such as ITO on the PI film, the direct printing method further reduces the thickness of the MA, which can achieve more flexibility, foldability, and conformability with the surface of complex irregular objects. The results show that the absorption rate of the designed MA exceeds 90% in the frequency range of 9.5–11.5 GHz. Due to the high symmetry of the resistance film structure, the MA is insensitive to polarization direction and incident angle.

The proposed MA in this work demonstrates tremendous potential in the field of flexible absorbers for practical applications and manufacturing processes. Utilizing a low-cost and easily fabricated intaglio printing technique, this MA exhibits notable advantages. Simultaneously, currently available flexible MAs face limitations in achieving significant bending effects, making it challenging to achieve higher degrees of folding and bending freedom. The flexible MA presented in this work stands out in this context by not only achieving a cer-

* Corresponding author: Huan Lu (luhuan123@zju.edu.cn).

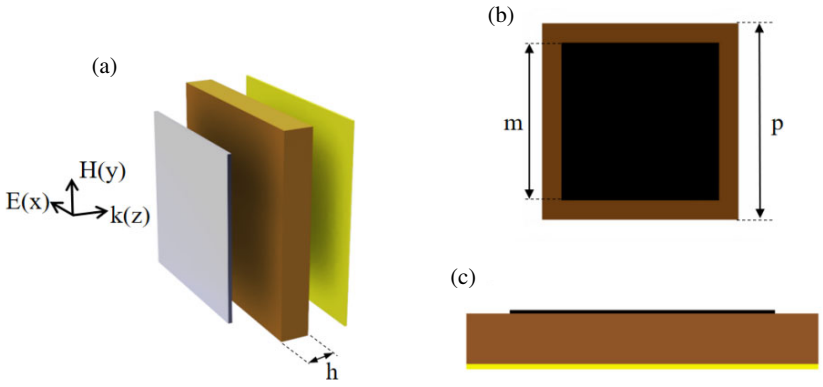

FIGURE 1. Schematic of the proposed MA. (a) Three-dimensional unit cell. (b) The top view of the unit cell. (c) The side view of the unit cell.

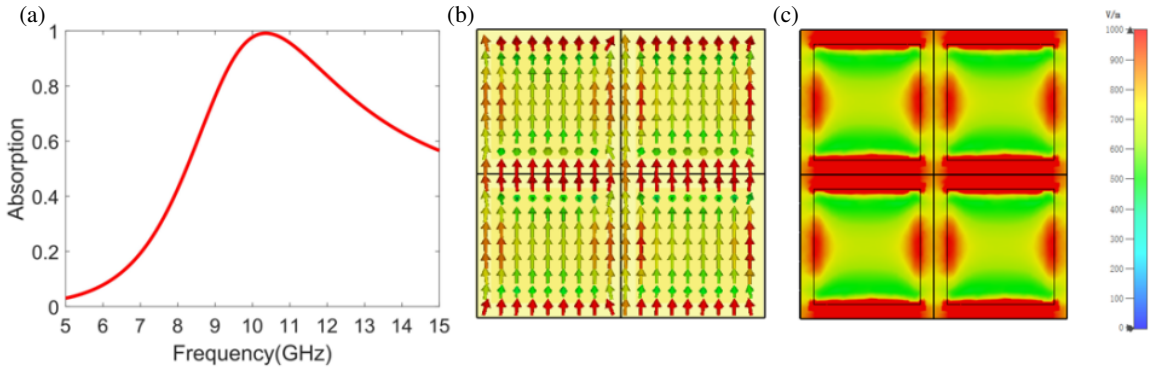

FIGURE 2. Simulation results. (a) Simulated absorption spectrum of proposed MA. (b) The surface current distribution of the conductive carbon paste ink layer. (c) Electric field distribution in conductive carbon paste ink resistance film.

tain degree of bending but, more importantly, aslo attaining a higher level of flexibility than existing flexible MAs, enabling a broader range of folding and bending. Moreover, because the flexible MA does not require any hard substrate or PI film, PET film intervention, the flexible effect is significantly better than the existing flexible MA, and the flexibility is comparable to that of flexible cloth. This characteristic makes the MA not only suitable for covering regular object surfaces but also capable of achieving conformal coverage on complex and irregular objects, providing an ideal solution for surfaces requiring absorptive properties with vast potential for practical applications. Additionally, the flexible MA exhibits outstanding durability, remaining resistant to damage and deformation during stretching processes, achieving a combination of lightweight and stability. Due to these properties, this MA is expected to have great potential in non-planar and conformal applications.

2. METAMATERIAL STRUCTURE AND METHODS

The proposed MA unit structure model is shown in Fig. 1. It consists of three layers, with a periodic square resistance film structure on the top, a flexible fabric dielectric substrate in the middle, and a continuous metal backplane at the bottom. As we all know, the structural design of metamaterials determines the properties of metamaterials, so the desired properties can be obtained by optimizing the structural parameters. Among them, the side length of the conductive carbon paste ink resistance film $m = 8\,\text{mm}$; the square resistance is $25\,\Omega/\square$; the thickness is about 10 microns; the thickness of the flexible fabric dielectric substrate $h = 1.43\,\text{mm}$; the dielectric constant is 2; the size of the unit cell $p = 10\,\text{mm}$; the thickness of the bottom copper layer $t = 0.035\,\text{mm}$; and the electrical conductivity is 5.8×10^7 S/m. The numerical simulation was performed using CST Microwave Studio software. Periodic boundary conditions were set in the x-y plane and the z-axis set to be open. The normal incident plane wave propagates along the z-direction, with the electric component along the y-direction and the magnetic field along the x-axis. Since the proposed MA is completely symmetric, the absorption efficiency of MA is insensitive to the normal incident polarization angle.

The absorption was calculated by $A(\omega) = 1 - R(\omega) - T(\omega)$, where $R(\omega) = |S_{11}|^2$ and $T(\omega) = |S_{21}|^2$ are the reflection and transmission, respectively. Since the metal backplane is located at the bottom of the MA structure, the transmission disappears, so the absorption expression can be simplified to $A(\omega) = 1 - R(\omega) = 1 - |S_{11}|^2$. The absorption spectrum of the simulation result is shown in Fig. 2(a). The simulation result shows that in the operating frequency band of 9.5–11.5 GHz, the absorption effect is above 90%; the FBW is 19%; and there is an absorption peak at 10.3 GHz.

In order to clarify the absorption mechanism of the design, the surface current distribution at the frequency point of the ab-

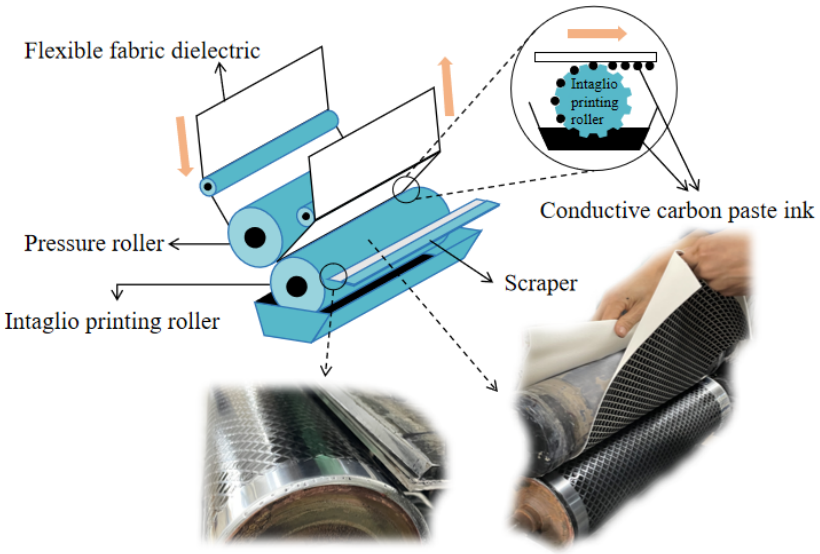

FIGURE 3. The picture of the intaglio printing machine.

sorption peak is monitored. The surface current distribution of the conductive carbon paste ink layer and the metal backplane corresponding to the absorption peak is shown in Fig. 2(b). The current mainly accumulates in the edge position of the square resistance film pattern, resulting in a strong electrical resonance. In addition, the current direction of the surface resistance film pattern and the bottom metal backplane reverse parallel to form a current loop, resulting in magnetic resonance in the structure. Due to the existence of conductive carbon paste resistance film, the surface current causes ohmic loss and converts EM energy into heat energy, which further expands the absorption bandwidth.

In order to clarify the source of loss, the energy loss of this frequency point is simulated, and the electric field size is drawn for visual analysis, as shown in Fig. 2(c). It can be seen that the energy loss mainly occurs in the surface resistance film, and the energy loss is similar to the surface current distribution and gathers at the edge of the square resistance film pattern, which proves that the electric field is strongly coupled with the edge of the square resistance film structure. Under the action of the electric field, a large number of charges gather at the edge of the square resistance film structure, causing a strong electrical response and playing a major role in the loss.

3. FABRICATION

The conductive carbon paste ink was printed by the traditional intaglio printing technology. The conductive carbon paste ink used is prepared by adding diluent and epoxy resin to the original carbon paste according to a specific concentration. The concentration ratio of specific square resistance values is obtained through a large number of concentration configuration experiments, and then multiple samples are configured according to each concentration ratio for testing. Compared with the traditional ITO resistance film that needs to be printed on a medium such as PI film, the advantage of this work is that specific concentrations of conductive carbon paste inks can be directly printed on a flexible fabric dielectric substrate through intaglio printing technology to achieve thinner and more flexible characteristics.

Roll-to-roll intaglio printing has become the mainstream technology for complex circuit printing because of its low cost, large area, and high-speed printing advantages, and it has better dimensional stability, durability, and pattern fidelity than inkjet printing and screen printing. In order to take advantage of these advantages of intaglio printing, the most important thing to print a specific pattern of resistance film is to configure a suitable conductive carbon paste ink. If the ink is too diluted, it will flow during the printing process and be difficult to shape, and if the ink is too thick, it will stick in the grooves on the roller, resulting in insufficient ink transfer to the surface of the flexible fabric medium. At the same time, the dilution and viscosity of the conductive carbon paste ink will affect the square resistance value of the printed resistance film. Through a lot of experiments, the concentration ratio of the conductive carbon paste ink stock, diluent, and epoxy resin corresponding to the square resistance value required by this work is obtained.

The first is the configuration of conductive carbon paste ink, 25 g conductive carbon paste ink paste, 6 g diluent, and 2 g epoxy resin mixed in a container and stirred evenly using a blender. As shown in Fig. 3, the intaglio printing machine is composed of three main parts: pressure roller, intaglio printing roller, and scraper. Turn on the intaglio press to rotate the roll, and at the same time, contact the clean scraper that has been wiped with the rotating intaglio roll at an appropriate angle. Then the configured conductive carbon paste ink is fully filled with the groove of the roller, and the excess ink on the surface of the intaglio roller is scraped with a scraper. Ideally, the area without a groove on the intaglio roller will not leave ink, but in fact, there will always be ink residue. After the ink is evenly scraped on the roller by the scraper, the pressure roller is pressed down to make the flexible fabric medium contact with the rotating intaglio roller, so that the ink in the groove of the roller is transferred to the flexible fabric medium.

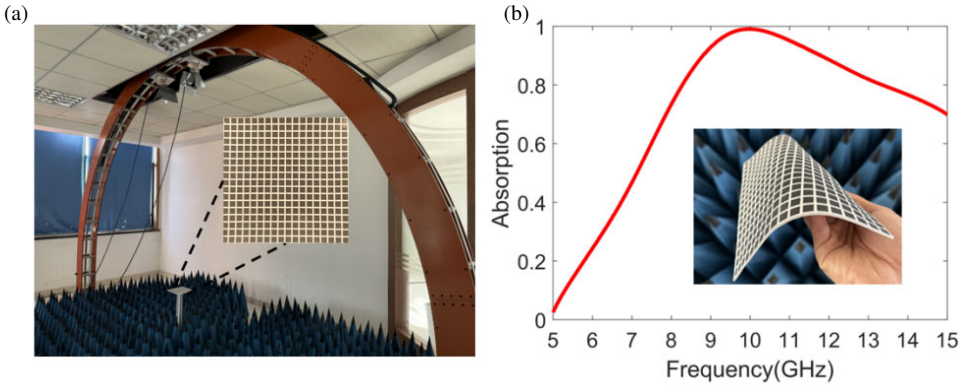

FIGURE 4. (a) Measurement setup for evaluating the performance of the MA. The metasurface is placed in an anechoic chamber. The transmitter and the probe are connected to the vector network analyzer. The transmitter is placed on an arch frame. The inset shows a schematic of the details of the sample. (b) Absorption spectrum of the experiment results and flexible sample.

4. RESULTS AND DISCUSSION

Several samples were prepared by intaglio printing. A pair of horns are connected to a vector network analyzer and placed on an arch in the laboratory to measure the reflection of the sample. As shown in Fig. 4(a), the reflection of copper plates of the same size at the same position was measured for comparison. Fig. 4(b) shows the absorption spectrum of the experimental results and flexible sample. We observed that the sample achieved more than 90% absorption rate in the range of 8.8–11.8 GHz, and the wave peak was near 10 GHz. Due to the use of epoxy resin in the manufacturing process, the conductive carbon paste resistance film printed on the surface of the sample can maintain its shape and electrical conductivity well in the bending, deformation, friction, and other processes of the flexible fabric medium, which is not easy to break and damage, fully reflecting the flexibility and foldability of the sample.

Compared with the simulation results, the frequency of the absorption peak is very similar, only slightly shifted to the low frequency, and the absorption frequency band has a certain degree of expansion. The experimental test results differ from the simulation ones within a specific range for the following reasons: Due to the slight thickness difference of the flexible fabric medium at different positions, the conductive carbon paste ink on the printing roller is not uniformly transferred to different positions of the flexible fabric in the process of intaglio printing, resulting in slight differences in the resistance of the resistance film square at different positions; secondly, because the thickness of the cloth medium is not uniform, the frequency band will be offset to a certain extent. Due to the above reasons, the prepared sample is equivalent to a metasurface composed of multiple similar structures with different parameters, and its overall absorption frequency band is equivalent to the combination of multiple frequency bands, so there is a certain deviation between the experimental and the simulated results.

Since the above are all reflected absorption results obtained under the vertical incidence of EM waves, but in the actual application scenario, EM waves will appear in oblique incidence, and maintaining good absorption stability at different incidence angles is an important indicator of MA. Therefore, we also simulated the changes in the absorption curve of the absorbing structure when the incidence angle increased from 0° to 60° under TE and TM polarizations, as shown in Figs. 5(a) and (b). As can be seen from Fig. 5(a), in TE polarization mode, when the incidence angle does not exceed 30°, the absorption rate is less affected by the incidence angle, and the absorption effect is stable. When the incidence angle is 45°, the absorption bandwidth is narrowed, but the absorption rate of more than 80% can still be maintained in the working band. According to Fig. 5(b), in the TM polarization mode, when the incidence angle does not exceed 30°, the absorption rate basically does not change and is little affected by the change of incidence angle. When the incidence angle is between 45° and 60°, the frequency point where the absorption peak is located will move to the high frequency, and the absorption rate will decrease to a certain extent, but there is still more than 80% absorption effect in a certain frequency range. By placing the horn antenna at different angles of the arch frame, we conducted experiments on the absorption effects of the samples at different incidence angles under TE and TM polarization modes, respectively. The experimental results are shown in Figs. 5(c) and (d). According to Fig. 5(c), it can be seen that in TE polarization mode, when the incidence angle does not exceed 30°, the absorption effect of the samples at different incidence angles will be greatly improved. The absorptivity is less affected by the change of incident angle and has a stable absorbing effect. When the incidence angle is 45°, the absorption bandwidth of more than 90% is narrowed, but the absorption rate of more than 80% can still be maintained in the working band. It can be seen from Fig. 5(d) that in TM polarization mode, when the incidence angle does not exceed 15°, the absorption rate basically does not change and is little affected by the change of incidence angle. When the incidence angle does not exceed 45°, the absorption band will move to high frequency, but there is still more than 90% absorption effect in a certain frequency range. The experimental results are basically consistent with the simulated ones. Through the analysis of the absorption curve of electromagnetic wave, it can be seen that the absorption rate of the absorption structure can be maintained at different polarization modes and different incident angles, and it has a good angle insensitive characteristic.

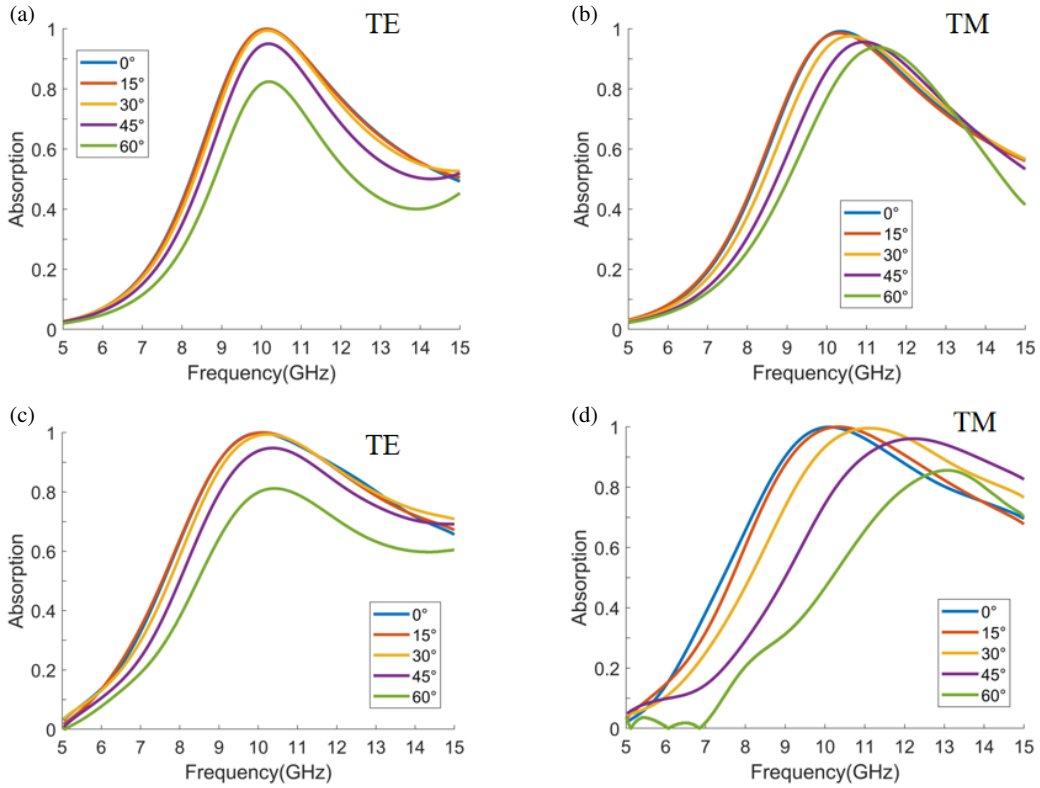

FIGURE 5. (a) Simulation results of absorption rate at different incidence angles in TE polarization mode. (b) Simulation results of absorption rate at different incidence angles in TM polarization mode. (c) Experimental results of absorption rate at different incidence angles in TE polarization mode. (d) Experimental results of absorption rate at different incidence angles in TM polarization mode.

5. CONCLUSIONS

In summary, a flexible foldable broadband MA prepared by intaglio printing technology is proposed. The absorber is composed of a conductive carbon paste ink resistance film, a flexible fabric medium and a metal backplane. Several samples were prepared by intaglio printing technology. Through simulation and experiments, it can be seen that the absorber can achieve more than 90% absorption in the range of 8.8–11.8 GHz; the FBW is 29%; and the polarization and incident angle is insensitive. These results indicate that the flexible wideband MA proposed by us is flexible, foldable, and capable of conformal covering on the surface of complex irregular objects, and can be applied to the commercial applications of a new generation of flexible, ultra-thin, ultra-wideband, wearable EM absorber in the near future.

ACKNOWLEDGEMENT

This work was sponsored by the National Natural Science Foundation of China (NNSFC) under Grant No. 62071423, the Natural Science Foundation of Zhejiang Province under Grant No. LQ21F050002 and No. LR23F010004, the Top-Notch Young Talent of Zhejiang Province, the Key Research and Development Program of Zhejiang Province under Grant No. 2024C01160, and the Postdoctoral Fellowship Program of CPSF under Grant No. GZB20230654.

REFERENCES

[1] Veselago, V. G., "The electrodynamics of substances with simultaneously negative values of ε and μ," *Soviet Physics Uspekhi*, Vol. 10, 509, 1968.

[2] Shelby, R. A., D. R. Smith, and S. Schultz, "Experimental verification of a negative index of refraction," *Science*, Vol. 292, No. 5514, 77–79, Apr. 2001.

[3] Schurig, D., J. J. Mock, B. J. Justice, S. A. Cummer, J. B. Pendry, A. F. Starr, and D. R. Smith, "Metamaterial electromagnetic cloak at microwave frequencies," *Science*, Vol. 314, No. 5801, 977–980, 2006.

[4] Marinov, K., A. D. Boardman, V. A. Fedotov, and N. Zheludev, "Toroidal metamaterial," *New Journal of Physics*, Vol. 9, No. 9, 324, 2007.

[5] Magnus, F., B. Wood, J. Moore, K. Morrison, G. Perkins, J. Fyson, M. C. K. Wiltshire, D. Caplin, L. F. Cohen, and J. B. Pendry, "A d.c. magnetic metamaterial," *Nature Materials*, Vol. 7, 295–297, 2008.

[6] Chen, H.-T., W. J. Padilla, J. M. O. Zide, A. C. Gossard, A. J. Taylor, and R. D. Averitt, "Active terahertz metamaterial devices," *Nature*, Vol. 444, 597–600, 2006.

[7] Huang, M., B. Zheng, T. Cai, X. Li, J. Liu, C. Qian, and H. Chen, "Machine-learning-enabled metasurface for direction of arrival estimation," *Nanophotonics*, Vol. 11, 2001–2010, 2022.

[8] Zhu, R., T. Chen, K. Wang, H. Wu, and H. Lu, "Metasurface-enabled electromagnetic illusion with generic algorithm," *Frontiers in Materials*, Vol. 10, 2023.

[9] Padilla, W. J., D. N. Basov, and D. R. Smith, "Negative refractive index metamaterials," *Materials Today*, Vol. 9, No. 7-8, 28–35,

2006.
[10] Dolling, G., M. Wegener, C. M. Soukoulis, and S. Linden, "Negative-index metamaterial at 780 nm wavelength," *Optics Letters*, Vol. 32, No. 1, 53–55, 2007.
[11] Chen, H. and M. Chen, "Flipping photons backward: Reversed Cherenkov radiation," *Materials Today*, Vol. 14, No. 1-2, 34–41, 2011.
[12] Duan, Z., X. Tang, Z. Wang, Y. Zhang, X. Chen, M. Chen, and Y. Gong, "Observation of the reversed Cherenkov radiation," *Nature Communications*, Vol. 8, 14901, 2017.
[13] Seddon, N. and T. Bearpark, "Observation of the inverse doppler effect," *Science*, Vol. 302, No. 5650, 1537–1540, 2003.
[14] Lee, S. H., C. M. Park, Y. M. Seo, and C. K. Kim, "Reversed Doppler effect in double negative metamaterials," *Physical Review B*, Vol. 81, 241102, Jun. 2010.
[15] Zhai, S. L., X. P. Zhao, S. Liu, F. L. Shen, L. L. Li, and C. R. Luo, "Inverse Doppler effects in broadband acoustic metamaterials," *Scientific Reports*, Vol. 6, 32388, 2016.
[16] Lu, H., B. Zheng, T. Cai, C. Qian, Y. Yang, Z. Wang, and H. Chen, "Frequency-controlled focusing using achromatic metasurface," *Advanced Optical Materials*, Vol. 9, No. 1, 2001311, Jan. 2021.
[17] Hu, Y., X. Liu, M. Jin, Y. Tang, X. Zhang, K. F. Li, Y. Zhao, G. Li, and J. Zhou, "Dielectric metasurface zone plate for the generation of focusing vortex beams," *PhotoniX*, Vol. 2, 10, Jun. 2021.
[18] Lu, H., J. Zhao, B. Zheng, C. Qian, T. Cai, E. Li, and H. Chen, "Eye accommodation-inspired neuro-metasurface focusing," *Nature Communications*, Vol. 14, No. 1, 3301, 2023.
[19] Lu, H., R. Zhu, C. Wang, T. Hua, S. Zhang, and T. Chen, "Soft actor-critic-driven adaptive focusing under obstacles," *Materials*, Vol. 16, No. 4, 1366, Feb. 2023.
[20] Landy, N. I., S. Sajuyigbe, J. J. Mock, D. R. Smith, and W. J. Padilla, "Perfect metamaterial absorber," *Physical Review Letters*, Vol. 100, 207402, 2008.
[21] Cheng, Y., H. Yang, Z. Cheng, and N. Wu, "Perfect metamaterial absorber based on a split-ring-cross resonator," *Applied Physics A*, Vol. 102, 99–103, 2011.
[22] Chen, H.-T., "Interference theory of metamaterial perfect absorbers," *Optics Express*, Vol. 20, No. 7, 7165–7172, 2012.
[23] Huang, L., D. R. Chowdhury, S. Ramani, M. T. Reiten, S.-N. Luo, A. K. Azad, A. J. Taylor, and H.-T. Chen, "Impact of resonator geometry and its coupling with ground plane on ultrathin metamaterial perfect absorbers," *Applied Physics Letters*, Vol. 101, 101102, 2012.
[24] Rhee, J. Y., Y. J. Yoo, K. W. Kim, Y. J. Kim, and Y. P. Lee, "Metamaterial-based perfect absorbers," *Journal of Electromagnetic Waves and Applications*, Vol. 28, 1541–1580, 2014.
[25] Zhao, X., K. Fan, J. Zhang, H. R. Seren, G. D. Metcalfe, M. Wraback, R. D. Averitt, and X. Zhang, "Optically tunable metamaterial perfect absorber on highly flexible substrate," *Sensors and Actuators A: Physical*, Vol. 231, 74–80, 2015.
[26] Bowen, P. T., A. Baron, and D. R. Smith, "Theory of patch-antenna metamaterial perfect absorbers," *Physical Review A*, Vol. 93, 063849, Jun. 2016.
[27] Lei, M., N. Feng, Q. Wang, Y. Hao, S. Huang, and K. Bi, "Magnetically tunable metamaterial perfect absorber," *Journal of Applied Physics*, Vol. 119, 244504, 2016.
[28] Liu, X., C. Lan, K. Bi, B. Li, Q. Zhao, and J. Zhou, "Dual band metamaterial perfect absorber based on Mie resonances," *Applied Physics Letters*, Vol. 109, No. 6, 062902, 2016.
[29] Khuyen, B. X., B. S. Tung, Y. J. Yoo, Y. J. Kim, K. W. Kim, L.-Y. Chen, V. D. Lam, and Y. Lee, "Miniaturization for ultra-thin metamaterial perfect absorber in the VHF band," *Scientific Reports*, Vol. 7, 45151, 2017.
[30] Schalch, J., G. Duan, X. Zhao, X. Zhang, and R. D. Averitt, "Terahertz metamaterial perfect absorber with continuously tunable air spacer layer," *Applied Physics Letters*, Vol. 113, No. 6, 061113, 2018.
[31] Liu, X., C. Lan, B. Li, Q. Zhao, and J. Zhou, "Dual band metamaterial perfect absorber based on artificial dielectric 'molecules'," *Scientific Reports*, Vol. 6, 28906, 2016.
[32] Amiri, M., F. Tofigh, N. Shariati, J. Lipman, and M. Abolhasan, "Review on metamaterial perfect absorbers and their applications to IoT," *IEEE Internet of Things Journal*, Vol. 8, No. 6, 4105–4131, 2021.
[33] Huang, M., B. Zheng, R. Li, X. Li, Y. Zou, T. Cai, and H. Chen, "Diffraction neural network for multi-source information of arrival sensing," *Laser & Photonics Reviews*, Vol. 17, No. 10, 2300202, 2023.
[34] Wu, G., X. Jiao, Y. Wang, Z. Zhao, Y. Wang, and J. Liu, "Ultra-wideband tunable metamaterial perfect absorber based on vanadium dioxide," *Optics Express*, Vol. 29, No. 2, 2703–2711, 2021.
[35] Zhu, R., D. Liu, H. Lu, L. Peng, T. Cai, and B. Zheng, "High-efficiency Pancharatnam-Berry metasurface-based surface plasma coupler," *Advanced Photonics Research*, 2300315, 2023.
[36] Zheng, B., H. Lu, C. Qian, D. Ye, Y. Luo, and H. Chen, "Revealing the transformation invariance of full-parameter omnidirectional invisibility cloaks," *Electromagnetic Science*, Vol. 1, No. 2, 1–7, 2023.
[37] Zhen, Z., C. Qian, Y. Jia, Z. Fan, R. Hao, T. Cai, B. Zheng, H. Chen, and E. Li, "Realizing transmitted metasurface cloak by a tandem neural network," *Photonics Research*, Vol. 9, No. 5, B229–B235, 2021.
[38] Li, R., Y. Jiang, R. Zhu, Y. Zou, L. Shen, and B. Zheng, "Design of ultra-thin underwater acoustic metasurface for broadband low-frequency diffuse reflection by deep neural networks," *Scientific Reports*, Vol. 12, No. 1, 12037, 2022.
[39] Banadaki, M. D., A. A. Heidari, and M. Nakhkash, "A metamaterial absorber with a new compact unit cell," *IEEE Antennas and Wireless Propagation Letters*, Vol. 17, No. 2, 205–208, 2018.
[40] Bhati, A., K. R. Hiremath, and V. Dixit, "Bandwidth enhancement of salisbury screen microwave absorber using wire metamaterial," *Microwave and Optical Technology Letters*, Vol. 60, No. 4, 891–897, 2018.
[41] Kim, J., H. Jeong, and S. Lim, "Mechanically actuated frequency reconfigurable metamaterial absorber," *Sensors and Actuators A: Physical*, Vol. 299, 111619, 2019.
[42] Long, L. V., N. S. Khiem, B. S. Tung, N. T. Tung, T. T. Giang, P. T. Son, B. X. Khuyen, V. D. Lam, L. Chen, H. Zheng, and Y. Lee, "Flexible broadband metamaterial perfect absorber based on graphene-conductive inks," *Photonics*, Vol. 8, No. 10, 2021.
[43] Lai, S., Y. Wu, J. Wang, W. Wu, and W. Gu, "Optical-transparent flexible broadband absorbers based on the ITO-PET-ITO structure," *Optical Materials Express*, Vol. 8, No. 6, 1585–1592, 2018.
[44] Park, S., G. Shin, H. Kim, Y. Kim, and I.-J. Yoon, "Polarization and incidence angle independent low-profile wideband metamaterial electromagnetic absorber using indium tin oxide (ITO) film," *Applied Sciences*, Vol. 11, No. 19, 9315, 2021.
[45] Yin, Z., Y. Lu, S. Gao, J. Yang, W. Lai, Z. Li, and G. Deng, "Optically transparent and single-band metamaterial absorber based on indium-tin-oxide," *International Journal of RF and Microwave Computer-Aided Engineering*, Vol. 29, No. 2, e21536, 2019.